Determination of Singlet Oxygen-Specific versus Radical-Mediated Lipid Peroxidation in Photosensitized Oxidation of Lipid Bilayers: Effect of β-Carotene and α-Tocopherol†

Steven P. Stratton and Daniel C. Liebler*

Department of Pharmacology and Toxicology, College of Pharmacy, University of Arizona, Tucson, Arizona 85721

Received April 14, 1997; Revised Manuscript Received July 24, 1997⊗

ABSTRACT: Photosensitized oxidation reactions damage tissue by catalyzing the formation of oxyradicals and singlet oxygen. β-Carotene is hypothesized to exert photoprotective effects by quenching singlet oxygen formed by Type II reactions and by scavenging free radicals formed by Type I reactions. β-Carotene antioxidant mechanisms were studied in a phospholipid membrane model of photooxidation with a new isotope dilution gas chromatography−mass spectrometry (GC-MS) assay that quantitatively distinguishes singlet oxygen-mediated and radical-mediated lipid peroxidation. This assay measures 9- and 10-hydroxylinoleate methyl esters and was used to generate photooxidation profiles for the photosensitizers methylene blue, Rose Bengal, and tetraphenylporphine. These profiles indicate a shift from Type II to Type I photooxidation mechanisms in later stages of photooxidation. β-Carotene (0.45 mol %) inhibited singlet oxygen-mediated lipid peroxidation at early stages of methylene blue-sensitized photooxidation. Production of radical-mediated products increased faster than singlet oxygen-mediated products at later stages. β-Carotene-5,8-endoperoxide, a specific marker for singlet oxygen oxidation of β-carotene in solution, was unstable under the incubation conditions and was not detected in this system. α-Tocopherol (0.45 mol %) was ineffective in inhibiting photosensitized lipid peroxidation, whereas 4.5 mol % α-tocopherol inhibited almost all radical-mediated lipid peroxidation as well as early-stage singlet oxygen-mediated lipid peroxidation. Cumene hydroperoxide stimulated radical-mediated lipid peroxidation, indicating that accumulation of hydroperoxides from Type II photooxidation may enhance Type I reactions. These data suggest that singlet oxygen quenching, rather than radical scavenging reactions, accounts for the photoprotective actions of β-carotene.

Photooxidation reactions are important in light-induced skin toxicity (Mathews-Roth et al., 1974) and photodynamic therapy of neoplastic disease (Sieber et al., 1984). On exposure to light, photosensitizers produce reactive oxygen species, which can subsequently react with lipids and other biomolecules [reviewed by Girotti (1990)]. Photosensitizers include dyes such as Rose Bengal and methylene blue; drugs such as tetracyclines, amiodarone, and chlorpromazine; polycyclic hydrocarbons found in coal tars; and endogenous porphyrins (Johnson & Ferguson, 1990; Halliwell & Gutteridge, 1989).

Excited photosensitizers can produce reactive oxygen species via two pathways. Absorption of light excites photosensitizers from ground state (S) to a triplet state (^{3}S) (eq 1). In Type I reactions, ^{3}S participates in electron transfer or hydrogen abstraction reactions with nearby molecules, followed by fast addition of oxygen to form peroxyl radicals (AOO•) (eq 2). In Type II reactions, ^{3}S can transfer its excitation energy to O_2 to form the nonradical singlet oxygen, a highly reactive excited-state form of molecular oxygen (eq 3). Free radicals formed in Type I reactions can initiate lipid peroxidation chain reactions. Singlet oxygen does not initiate lipid peroxidation chain reactions, but it can react with unsaturated phospholipid to form lipid hydroperoxides that contribute to chain reaction initiation in the presence of transition metals (Dix & Aikens, 1993).

$$S \xrightarrow{h\nu} {}^3S \tag{1}$$

$${}^3S + A \xrightarrow{-e^-,\,-H} A^\bullet \xrightarrow{O_2} AOO^\bullet \tag{2}$$

$${}^3S + O_2 \rightarrow S + {}^1O_2 \tag{3}$$

Distinguishing between Type I and Type II photooxidative mechanisms can be done, in principle, on the basis of analyses of specific lipid oxidation products. Photooxidation of DLPC[1] liposomes results in peroxidation of the linoleoyl moieties of DLPC. Radical-mediated (Type I) photooxidation reactions form equal amounts of hydroperoxides at the 9′ and 13′ positions, whereas singlet oxygen-mediated (Type

† This work was supported by USPHS Grants CA56875 and ES06694.

* Author to whom correspondence should be addressed. Fax (520) 626-2466; E-mail liebler@pharmacy.arizona.edu.

⊗ Abstract published in *Advance ACS Abstracts,* October 1, 1997.

[1] Abbreviations: DLPC, 1,2-dilinoleoyl-*sn*-glycero-3-phosphocholine; BHT, 2,6-di-*tert*-butyl-4-methylphenol; TPP, tetraphenylporphine; RB, Rose Bengal; RBTEA, Rose Bengal *bis*(triethylammonium) salt; BSTFA, *bis*(trimethylsilyl)trifluoroacetamide; TMCS, trimethylchlorosilane; FID, flame ionization detection; 9-OH MeLin, 9-hydroxylinoleate methyl ester; 10-OH MeLin, 10-hydroxylinoleate methyl ester; 12-OH MeLin, 12-hydroxylinoleate methyl ester; 13-OH MeLin, 13-hydroxylinoleate methyl ester; TMS, trimethylsilyl; APCI, atmospheric pressure chemical ionization; 9′-OOH, 9′-hydroperoxy-1,2-dilinoleoyl-*sn*-glycero-3-phosphocholine; 10′-OOH, 10′-hydroperoxy-1,2-dilinoleoyl-*sn*-glycero-3-phosphocholine; 12′-OOH, 12′-hydroperoxy-1,2-dilinoleoyl-*sn*-glycero-3-phosphocholine; 13′-OOH, 13′-hydroperoxy-1,2-dilinoleoyl-*sn*-glycero-3-phosphocholine.

S0006-2960(97)00864-7 CCC: $14.00

Scheme 1: Photooxidation of Linoleoyl Groups in Phospholipids Forms Hydroperoxides[a]

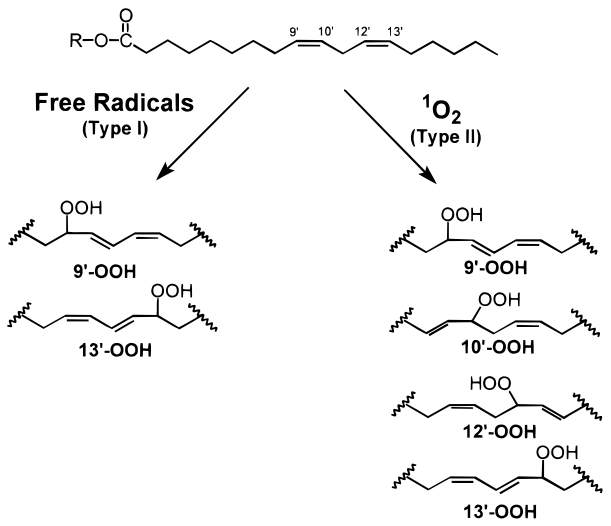

[a] Singlet oxygen oxidation adds -OOH at either 9′, 10′, 12′, or 13′ positions. Oxygen radical attack forms only the conjugated dienyl 9′- and 13′-hydroperoxides.

II) photooxidation reactions form equal amounts of hydroperoxides at the 9′, 10′, 12′, and 13′ positions (Scheme 1) (Terao et al., 1981; Girotti, 1990). Since each pathway forms equal amounts of the respective isomers, measurement of 9′-OOH or 13′-OOH linoleoyl side chains provides an index of nonspecific photooxidation, whereas measurement of 10′-OOH or 12′-OOH linoleoyl chains provides an index of singlet oxygen-specific (Type II) photooxidation.

To quantitatively distinguish photooxidation reaction pathways, we have developed a sensitive assay for these products based on isotope dilution GC-MS. We developed these methods to further our studies of the antioxidant actions of β-carotene (Stratton et al., 1993; Kennedy & Liebler, 1991, 1992), which is a highly effective protectant *in vivo* against photodamage associated with erythropoetic protoporphyria (Mathews-Roth, 1993). A very effective singlet oxygen quencher, β-carotene quenches singlet oxygen-induced damage catalytically by a physical mechanism (Foote & Denny, 1968) and by a chemical mechanism that results in the formation of β-carotene oxidation products (Stratton et al., 1993). As a free radical scavenger, however, the efficiency of β-carotene varies with pO_2 (Burton & Ingold, 1984). At low pO_2, β-carotene has antioxidant behavior that is lost as pO_2 increases. β-Carotene readily autoxidizes at high pO_2, and may even act as a prooxidant. Recent studies in our laboratory (Liebler et al., 1997) indicate that the effectiveness of β-carotene as a chain-breaking antioxidant *in vitro* is highly dependent on the conditions of the experimental system. In biological membranes containing comparable amounts of β-carotene and α-tocopherol, the latter exerted the predominant antioxidant effect. Although the photoprotective action of β-carotene could involve either singlet oxygen quenching or radical scavenging, the effects of antioxidants on these competing photooxidation processes have not previously been quantified.

The goals of this study were to characterize the contributions of Type I and Type II processes to photosensitized lipid peroxidation in DLPC liposomes and to assess the effects of the antioxidants β-carotene and α-tocopherol on Type I and Type II-mediated photooxidation. These effects were measured with a new GC-MS assay that quantitatively distinguishes between singlet oxygen-specific and nonspecific lipid peroxidation products. We also attempted to monitor the formation of β-carotene-5,8-endoperoxide, a major product and specific marker for singlet oxygen quenching by β-carotene in solution (Stratton et al., 1993). While this product is a potential marker for this activity in more complex biological systems, LC-MS analysis indicated it was not formed in detectable amounts in this liposome system.

EXPERIMENTAL PROCEDURES

Chemicals and Instrumentation. 1,2-Dilinoleoyl-*sn*-glycero-3-phosphocholine (Avanti Polar Lipids, Alabaster, AL), linoleate methyl ester (Nu-Chek Prep, Elysian, MN), and methanol-d_4 (Cambridge Isotope Laboratories, Andover, MA) were used as received. β-Carotene and 12-hydroxylauric acid were from Fluka (Ronkonkoma, NY). Methylene blue, cumene hydroperoxide, and BHT were from Sigma (St. Louis, MO). NaH (60% in mineral oil), $NaBH_4$, TPP, RB, RBTEA (dye content 90%), propionic anhydride, and platinum oxide were from Aldrich (Milwaukee, WI). BSTFA + 1% TMCS was from Pierce (Rockford, IL). α-Tocopherol-*d* was a gift from Henkel Fine Chemicals (La Grange, IL). Methyl 12-hydroxylaurate was prepared via treatment of 12-hydroxylauric acid with ethereal diazomethane. α-Tocopherol propionate was prepared by esterification of α-tocopherol with propionic anhydride according to the general method of Baxter et al. (1943). All other reagents and solvents were of the highest grade of purity available and were used as received. HPLC analyses were done with a Hewlett-Packard Model 1050 four-channel gradient pump and 1040M diode-array detector system controlled with HP ChemStation software. GC-MS analyses were done with a Fisons MD800 mass spectrometer coupled to a Carlo Erba 5000 series GC (Fisons Instruments, Beverly, MA). GC-FID analyses were done with a Hewlett-Packard 5890 series gas chromatograph controlled with HP ChemStation software. HPLC-MS analyses were done with a Finnigan TSQ7000 triple-quadrupole instrument (Finnigan MAT, San Jose, CA), equipped with a DEC 3000 Alpha work station, a Finnigan APCI source, and a Hewlett-Packard 1050 HPLC system.

Preparation of 9- and 10-OH MeLin Standards. Preparation of 9-OH MeLin and 10-OH MeLin was based on the method of Terao et al. (1981). Linoleate methyl ester (100 mg, 340 μmol) and methylene blue (1.6 mg, 5 μmol) were dissolved in 50 mL of methanol. This solution was bubbled with O_2 in a jacketed borosilicate glass flask and illuminated with a 300-W tungsten−halogen lamp at a distance of 15 cm for 12 h at 25 °C. Solvent was evaporated *in vacuo*. The product residue was treated with 10 mg of $NaBH_4$ in 3 mL of methanol for 30 min at room temperature to reduce lipid hydroperoxides to lipid alcohols. H_2O (3 mL) and 10 drops of HCl (2 M) were added to the reaction mixture and lipid was extracted with an equal volume of hexane/2-propanol (3:2 v/v). Linoleate methyl ester and its hydroxides were separated by normal-phase HPLC on a 5-μm Spherisorb silica column (4.6 × 250 mm), eluted with hexane/2-propanol/acetic acid (99:1:0.1 v/v/v) delivered at 1.0 mL min^{-1}. Products eluting at 12.7 and 14.2 min were identified as 10-OH MeLin and 9-OH MeLin, respectively, by GC-MS analysis (described below). These products were collected and repurified by HPLC as above.

Preparation of 9- and 10-OH MeLin-d_3 Internal Standards. Deuterated internal standards were prepared by transesterification of 9- and 10-OH MeLin with methanol-d_4. Purified hydroxylinoleate methyl ester compounds collected above were dissolved separately in 1 mL of methanol-d_4, added to approximately 10 mg of NaH, and incubated for 30 min at room temperature. Potassium phosphate buffer (3 mL, pH 7.0, 2 M) was added and lipids were extracted with an equal volume of hexane/2-propanol (3:2 v/v). Solvent was removed *in vacuo* and deuterated lipids were stored in hexane at −20 °C. Synthesis and recovery of deuterated products were confirmed by GC-MS analysis (described below).

Quantification of Hydroxylinoleate Methyl Ester Standards by GC-FID. A standard curve was prepared from dilutions of pure 9-OH MeLin [quantified by UV−vis, $\epsilon = 25{,}900$ M^{-1} in hexane (Chan & Levett, 1977)] ranging from 20 to 200 ng of the standard injected and containing 21 ng of internal standard methyl 12-hydroxylaurate. Samples were derivatized to form TMS ethers and injected on-column onto a 20 m × 0.53 mm i.d. DB-5 capillary column (J & W Scientific, Folsom, CA) with helium as the carrier gas and were detected with flame ionization. The GC oven temperature was 100 °C for 2 min, then programmed to 280 °C at 15 °C min^{-1}, and held at 280 °C for 6 min. The detector temperature was 250 °C. Stock solutions of 10-OH MeLin, 9-OH MeLin-d_3, and 10-OH MeLin-d_3 were standardized by similar GC-FID analysis of aliquots calibrated with the 9-OH MeLin standard curve. Since 9-O-TMS, 10-O-TMS, 9-*O*-TMS-d_3, and 10-O-TMS-d_3 ethers of linoleate methyl ester are positional isomers, GC-FID response factors of each were assumed to be equal, within experimental error. TMS derivatization of hydroxylinoleate methyl ester isomers was confirmed with parallel analysis by GC-MS (data not shown).

Liposome Photooxidation and Extraction. A gentle stream of N_2 was used to remove solvent and form a thin film of DLPC (10 mg, 12.8 μmol) in a silanized round-bottom flask. In experiments where photosensitizer was incorporated into the lipid bilayer, 0.50 μmol of TPP or RBTEA was added prior to solvent removal. Some preparations contained β-carotene, β-carotene-5,8-endoperoxide, or α-tocopherol incorporated into the liposome membrane. In these experiments, compounds were mixed with DLPC and solvent was removed with a gentle stream of N_2 prior to liposome formation. In experiments with cumene hydroperoxide, this compound was diluted in methanol (286 μM) and added to the buffer prior to liposome formation. Liposomes were formed by vortex-mixing the contents of the flask for 60 s in 10 mL of Chelex-treated buffer (50 mM Tris-HCl and 100 mM NaCl, pH 7.0) followed by bath sonication for 3 min. The mixture then was transferred to a 50 mL 3-neck pear-shaped flask suspended in a 37 °C H_2O bath. The side necks were connected to a reflux condenser (cooled with chilled H_2O to prevent evaporation of buffer) and an O_2 inlet tube. Liposomes were bubbled with O_2 under illumination provided by a 300-W tungsten−halogen lamp at a distance of 15 cm. Aliquots (1 mL) were removed through the center neck at various time points. In experiments where photosensitizer was added directly to liposomes, 50 μL of RB (0.01 M in H_2O) or methylene blue (0.01 M in methanol) was added immediately prior to illumination.

Lipid Extraction, $NaBH_4$ Reduction, and Transesterification. Liposome samples were extracted with equal volumes of ethyl acetate containing BHT (22 μg, 100 nmol) to prevent adventitious oxidation during treatment. Samples were dissolved in 1.5 mL of methanol and treated with 5 mg of $NaBH_4$ for 30 min at room temperature. Then 3 mL of H_2O and 10 drops of HCl (2 M) were added to the reaction mixture and the lipid was extracted with an equal volume of hexane/2-propanol (3:2 v/v). The solvent was evaporated with a gentle stream of N_2 and samples were redissolved in 1 mL of KOH/methanol (100 mg/mL) for 10 min at room temperature, followed by addition of 2 mL of potassium phosphate buffer (pH 7, 2 M). Samples were extracted with an equal volume of hexane/2-propanol (3:2 v/v) and transferred to silanized 1.5 mL screw-cap autosampler vials.

Lipid Derivatization and Catalytic Hydrogenation. Prior to derivatization, 25 nmol of 9- and 10-OH MeLin-d_3 internal standards were added to each vial. TMS ethers were prepared by addition of 100 μL of BSTFA + 1% TMCS to samples, which were sealed with a Teflon-lined cap and heated for 45 min at 65 °C. After heating, samples were evaporated with a gentle stream of N_2 and redissolved in 0.5 mL of distilled ethyl acetate. Platinum oxide (3 mg) was added to each vial and samples were purged with H_2 for 2 min to reduce samples to TMS ethers of stearate methyl ester. Solvent was evaporated with a gentle stream of N_2 and samples were immediately redissolved in 0.5 mL of toluene for GC-MS analysis. The platinum catalyst settled to the bottom of the vial and did not interfere with sample injection. For standard curves, mixtures of standard 9- and 10-OH MeLin (1−100 pmol) were carried through the derivatization/hydrogenation procedure described above.

GC-MS Analysis of Products. TMS derivatives of lipid oxidation products were injected on-column with a Fisons A200S autosampler, separated on a 30 m × 0.25 mm i.d. DB-5ms capillary column (J & W Scientific, Folsom, CA) with helium as the carrier gas, and ionized with a 70-eV electron beam. The GC oven temperature was 100 °C for 2 min, then programmed to 280 °C at 15 °C min^{-1}, and held at 280 °C for 2 min. The transfer line and source were maintained at 250 and 200 °C, respectively. Some samples were monitored in the selected ion mode at *m/z* ratios for characteristic fragment ions of 9- and 10-O-TMS stearate methyl ester and their corresponding trideuterolabeled internal standards. Levels of these products were determined with calibration curves prepared from known amounts of 9- and 10-O-TMS stearate methyl ester plus their deuterated analogs as internal standards. α-Tocopherol depletion from photooxidized liposomes was also measured by isotope dilution GC-MS according to the method of Liebler et al. (1996), with hexadeuterolabeled α-tocopherol as an internal standard.

Synthesis of β-Carotene-5,8-endoperoxide. β-Carotene-5,8-endoperoxide was prepared by singlet oxygen oxidation of β-carotene with methylene blue. β-Carotene (1.6 mg, 3.0 μmol) and methylene blue (1.3 mg, 4.1 μmol) were dissolved in 50 mL of toluene. This solution was bubbled with O_2 in a jacketed borosilicate glass flask and illuminated with a 300-W tungsten−halogen lamp at a distance of 15 cm for 2 h at 5 °C. Solvent was evaporated *in vacuo*, and carotenoids were separated from the product residue via differential solubility in hexane. Solvent was evaporated *in vacuo*, and the product residue was dissolved in mobile phase for purification by HPLC, according to the method of Stratton et al. (1993). All products were handled under reduced light.

HPLC Analysis of Carotenoid Depletion. Liposome samples containing β-carotene or β-carotene-5,8-endoperoxide were extracted as described above. Extraction of the liposomes indicated that recovery of β-carotene was >90% of the expected level, which indicates that at least 90% of the added carotenoid was incorporated into the lipid bilayer (data not shown). With 22 nmol of α-tocopherol propionate as an injection internal standard, samples were analyzed by reverse-phase HPLC on a 5 μm Spherisorb ODS-2 column (4.6 × 250 mm), eluted with methanol/hexane (90:10 v/v) delivered at 1.5 mL min^{-1}.

LC-MS Analysis of β-Carotene-5,8-endoperoxide. DLPC liposomes containing 0.45 mol % β-carotene were photooxidized and sampled at various timepoints. Samples were extracted as described above and aliquots were analyzed for β-carotene-5,8-endoperoxide by reverse-phase LC-MS. Samples were injected onto a 5 μm Spherisorb ODS-2 column (4.6 × 250 mm) and eluted with methanol/hexane (90:10 v/v) at 1.5 mL min^{-1}. Column effluent was directed through a UV−vis detector and then into the APCI source.

RESULTS

Analysis of DLPC Photosensitized Oxidation. The compounds 9′-OOH linoleate and 10′-OOH linoleate are markers of nonspecific and singlet oxygen-mediated photooxidation, respectively, in DLPC liposomes. Analysis of the intact phospholipid hydroperoxide by GC-MS is precluded by thermal instability and lack of volatility of the phospholipid hydroperoxides. Alternatively, rigorous quantitative HPLC analysis of the phospholipid hydroperoxide poses the daunting challenge of synthesizing chemically defined standard phospholipid hydroperoxides and working with these highly unstable compounds. We have elected to analyze the 9- and 10-OOH linoleate moieties as O-TMS derivatives of their corresponding hydroxystearate methyl esters. As described under Experimental Procedures, the analysis involves (1) $NaBH_4$ reduction of the phospholipid hydroperoxides to alcohols, (2) transesterification of the phospholipid to hydroxylinoleate methyl esters, (3) silylation of the 9- and 10-hydroxy functions, and (4) catalytic hydrogenation to produce the corresponding 9-O-TMS and 10-O-TMS stearate methyl ester derivatives.

The isotope dilution GC-MS approach employed here requires high-purity analytical standards for instrument calibration curves, as well as deuterated analogues for all analyses. Because these materials were not commercially available, we synthesized and standardized the 9- and 10-hydroxylinoleate methyl esters as described under Experimental Procedures. These were synthesized by the methylene blue-sensitized photooxidation of linoleate methyl ester. Normal-phase HPLC analysis of the oxidation products (Figure 1) indicated that 12- and 13-OH MeLin were not separated by this system, whereas 9- and 10-OH MeLin were well-resolved. Because of this difficulty in purifying 12- and 13-OH MeLin, we focused exclusively on analyses of 9- and 10-OH MeLin. MS data for the O-TMS derivatives of 9- and 10-OH MeLin and their deuterated analogues are presented in Table 1. Fragmentation of the 9-O-TMS derivative is consistent with previously reported data (Hughes et al., 1983; Hubbard et al., 1980).

Time Course Study of Liposome Photooxidation with Various Photosensitizers. Photooxidation of DLPC liposomes occurs via two reaction pathways. Type I photooxidation is radical-mediated and forms hydroperoxides at the 9′ position on the linoleoyl moiety. Type II photooxidation is singlet oxygen-mediated and forms hydroperoxides at both the 9′ and 10′ positions. Thus, 10′-OOH is a marker for singlet oxygen-specific lipid peroxidation, whereas 9′-OOH indicates oxidation by both singlet oxygen and radicals. The contribution of radicals to lipid peroxidation is simply the difference between levels of 9′-OOH and 10′-OOH. Lipid peroxidation was measured over a 4 h period in liposomes photooxidized with the photosensitizers methylene blue, RB, RBTEA, and TPP (Figure 2). Solubility of the lipophilic photosensitizers RBTEA and TPP is poor in aqueous buffer. Since photooxidation may partially depend on the proximity of the photosensitizer to the membrane (Kochevar et al., 1996; Krinsky, 1979), these photosensitizers were incorporated directly into the lipid bilayer during liposome preparation. Methylene blue and RB were soluble in the buffer and were added after the liposomes were formed (see Experimental Procedures).

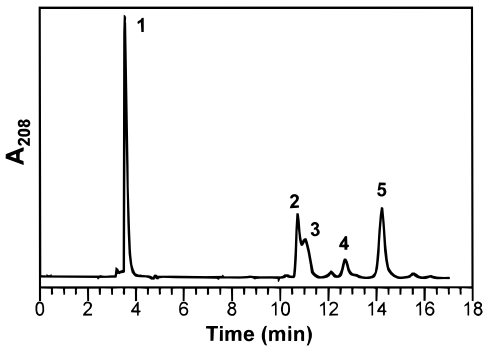

FIGURE 1: Normal-phase HPLC chromatogram of linoleate methyl ester photooxidation products showing linoleate methyl ester (**1**) and oxidation products 13-OH MeLin (**2**), 12-OH MeLin (**3**), 10-OH MeLin (**4**), and 9-OH MeLin (**5**).

Photooxidation of DLPC liposomes with the different photosensitizers produced very different oxidation profiles. In methylene blue-sensitized photooxidation, production of 9′- and 10′-OOH was identical for the first 75 min (early stages) of the reaction. From 75 to 180 min (late stages), levels of 9′-OOH increased, whereas those of 10′-OOH declined. From the data shown in Figure 2, it is apparent that radical-mediated processes surpass singlet oxygen-mediated oxidation after initial stages of photooxidation. The decrease in product levels after 180 min (very late stages) was not unexpected, as the products of interest can undergo secondary oxidations to other compounds (Loidl-Stahlhofen et al., 1994), which are not detected in this assay. In TPP-sensitized photooxidation, levels of 10′-OOH did not parallel levels of 9′-OOH as they did in the methylene blue-photosensitized oxidation, indicating that Type II mechanisms make a smaller contribution to total lipid peroxidation in TPP-sensitized photooxidations.

In liposomes photooxidized with RBTEA and RB, products were not seen after 30 min. However, these photosensitizers were rapidly bleached as compared to methylene blue and TPP. Visible coloration of the liposomes was virtually absent by 75 min. More photooxidation occurred with RBTEA than with RB, though this may reflect differences in their respective locations in the liposome mixture.

Effect of Antioxidants on Type I vs Type II Photooxidation in DLPC Liposomes. In our studies with the liposome model,

Table 1: Electron-Ionization Mass Spectra of 9-OH MeLin, 10-OH MeLin, and Their Trideuterolabeled Analogs[a]

product	peak no.[b]	*m/z* (rel abundance)
9-O-TMS linoleate methyl ester	5	382 ($M^{+\bullet}$, 2%), 311 (5), 225 (61), 143 (19), 130 (28), 73 (100)
9-O-TMS-d_3 linoleate methyl ester		385 ($M^{+\bullet}$, 4%), 314 (6), 225 (66), 143 (20), 130 (28), 73 (100)
10-O-TMS linoleate methyl ester	4	271 (100%), 149 (20), 129 (31), 121 (18), 73 (77)
10-O-TMS-d_3 linoleate methyl ester		274 (85%), 149 (19), 129 (32), 121 (18), 73 (100)

[a] Products were derivatized to linoleate methyl ester-TMS ethers prior to analysis as described in Experimental Procedures. [b] Linoleate methyl ester photooxidation product peak isolated by HPLC (Figure 1).

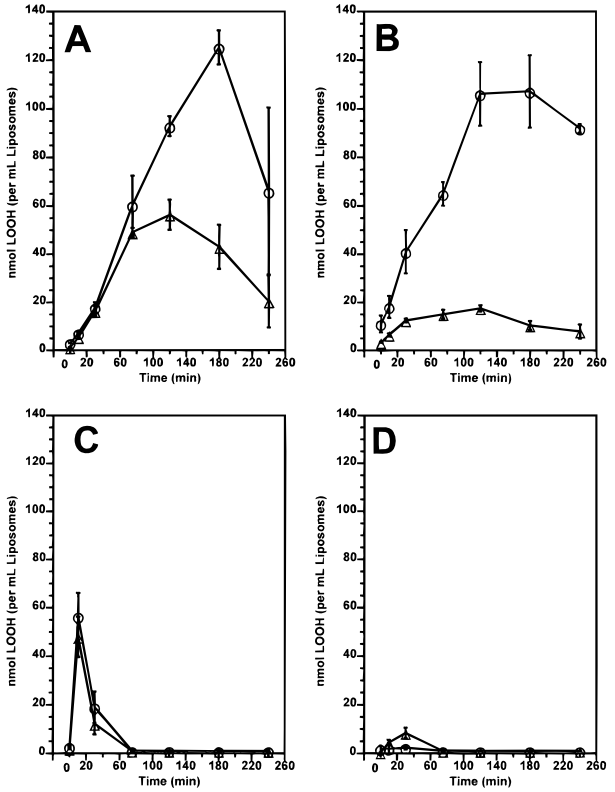

FIGURE 2: Effects of the photosensitizers methylene blue (A), TPP (B), RBTEA (C), and RB (D) on production of 9′-OOH (○) and 10′-OOH (△) in photooxidized DLPC liposomes. TPP and RBTEA were incorporated into the liposome bilayer, whereas methylene blue and RB were added to the mixture immediately prior to illumination of the liposomes. Results are expressed as mean ± SD ($n = 3$).

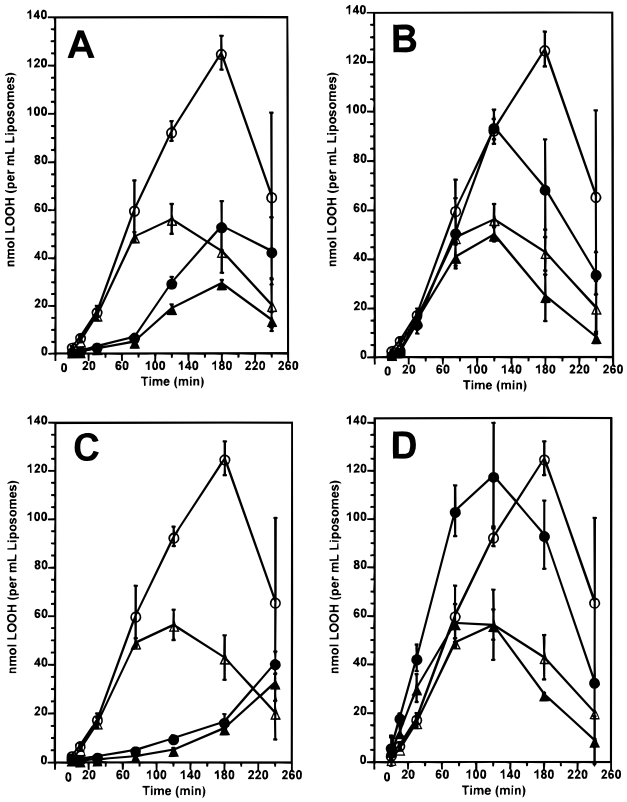

FIGURE 3: Effects of antioxidants on photosensitized peroxidation of liposomes. DLPC liposomes were photooxidized with methylene blue, extracted, and analyzed by GC-MS as described in Experimental Procedures. 9′-OOH (○) and 10′-OOH (△) indicate levels of nonspecific and singlet oxygen-specific photooxidation, respectively, in the presence (filled symbols) and absence (open symbols) of 0.45 mol % β-carotene (A), 0.45 mol % α-tocopherol (B), 4.5 mol % α-tocopherol (C), and 0.45 mol % cumene hydroperoxide (D). Results are expressed as mean ± SD ($n = 3$). Data for methylene blue-sensitized oxidation without additives (open symbols) are reproduced from Figure 2A for purposes of comparison.

we employed β-carotene at a concentration of 0.45 mol %, on the basis of phospholipid. This concentration of β-carotene was chosen based on previous studies that showed liposomes containing more than 0.5 mol % β-carotene are difficult to prepare since β-carotene tends to crystallize out in the aqueous buffer during sonication (Kennedy & Liebler, 1992). Studies in our laboratory showed that microsomes from Mongolian gerbils supplemented 6 weeks with 0.1% dietary β-carotene contain 0.21 mol % β-carotene based on phosphate levels (Liebler et al., 1997). The effect of β-carotene on methylene blue-sensitized photooxidation of DLPC liposomes is shown in Figure 3A. β-Carotene significantly inhibited early-stage lipid peroxidation for the first 75 min (Table 2). This was followed by an increase in products from 75 to 180 min. After 75 min, levels of 9′-OOH increased faster than 10′-OOH. This divergence in the product curves following early-stage lipid peroxidation indicates an increasing contribution of radical-mediated processes at later stages of lipid peroxidation.

β-Carotene is an excellent singlet oxygen quencher but a poor free radical-trapping antioxidant under conditions of high pO_2, as in our experiments (Kennedy & Liebler, 1992; Burton & Ingold, 1984). This is in contrast to α-tocopherol, which is less effective as a singlet oxygen quencher but a better free radical scavenger at high pO_2, as in this experiment (Foote, 1979; Burton & Ingold, 1984). β-Carotene inhibited both nonspecific and singlet oxygen-mediated photooxidation, indicating that methylene blue photooxidation occurs via mainly a Type II mechanism, at least in initial stages. To test this assumption, the effect of 0.45 mol % α-tocopherol on methylene blue-sensitized photooxidation of DLPC liposomes was measured (Figure 3B). Early-stage production of 9′- and 10′-OOH was not significantly altered in the presence of α-tocopherol as compared to photooxidized control liposomes (Table 2). A divergence in 9′- and 10′-OOH production was observed after 75 min in both control and α-tocopherol-containing liposomes, indicating increasing Type I photooxidation with time in this system. The lack

Table 2: Effect of Various Agents on Rates of LOOH Isomer Production in DLPC Liposomes Photooxidized with Methylene Blue[a]

agent	concentration	9′-OOH	10′-OOH[b]
control		0.780 ± 0.168	0.648 ± 0.026
β-carotene	0.45 mol %	0.082 ± 0.016[b]	0.058 ± 0.013[b]
α-tocopherol	0.45 mol %	0.693 ± 0.190	0.546 ± 0.067
β-carotene + α-tocopherol	0.45 mol %	0.277 ± 0.076[b]	0.233 ± 0.084[b]
α-tocopherol	4.5 mol %	0.044 ± 0.012[b]	0.018 ± 0.008[b]
cumene hydroperoxide	5.8 μM	1.30 ± 0.190[b]	0.696 ± 0.105

[a] Rates (nanomoles per milliliter per minute) calculated on the basis of linear portion of photooxidation vs time curves (0−75 min). Results are expressed as mean ± SD ($n = 3$). [b] Significant differences between rates of production of respective LOOH isomers as compared to control (DLPC liposomes photooxidized with methylene blue alone) based on Student's *t*-test (two-tailed, $p < 0.05$).

of inhibition of radical-mediated photooxidation appears to be due to rapid consumption of α-tocopherol by singlet oxygen in early stages (see below). However, when DLPC liposomes were photooxidized in the presence of both β-carotene and α-tocopherol (0.45 mol %), the rates of product formation were greater than with β-carotene alone (Table 2).

To test the effect of a higher α-tocopherol concentration, the experiment was repeated with 4.5 mol % α-tocopherol (Figure 3C). This level of α-tocopherol caused a significant lag in formation of both 9′- and 10′-OOH for the first 3 h as compared to control liposomes. After 75 min, there was a parallel time-dependent increase in both products, indicating that lipid peroxidation is occurring via a Type II mechanism. In contrast to experiments with β-carotene, levels of 9′-OOH did not increase faster than 10′-OOH following the lag in formation. This indicates that radical-mediated photooxidation processes were suppressed by this supraphysiological level of α-tocopherol, even in later stages of lipid peroxidation.

Antioxidant Depletion during Liposome Photooxidation. Photooxidative processes can result in the destruction of β-carotene and α-tocopherol by autoxidation, antioxidant activity, or chemical quenching of singlet oxygen. Levels of β-carotene and α-tocopherol were measured during the course of photooxidation to study their depletion over time. Depletion of β-carotene in photooxidized DLPC liposomes was analyzed by HPLC (Figure 4). Photooxidation resulted in depletion of ∼35% of the β-carotene at 75 min, with >40% still remaining after 4 h. The presence of equimolar α-tocopherol did not affect the depletion kinetics of β-carotene.

An equivalent level of α-tocopherol was much less effective than β-carotene in inhibiting photooxidative damage in these experiments. To test the stability of α-tocopherol in this system, depletion was measured by GC-MS (Figure 5). α-Tocopherol was rapidly consumed in this system, even in the presence of equimolar β-carotene or at a 10-fold higher concentrations (4.5 mol %). When DLPC liposomes containing 0.45 mol % α-tocopherol were photooxidized (with or without β-carotene), 90% of the α-tocopherol was depleted by 75 min. Only a slight protective effect of β-carotene on α-tocopherol depletion was observed from 30 to 75 min. The slopes of the curves in Figure 5 indicate that the consumption of α-tocopherol was slightly slower in liposomes containing the higher concentration of α-tocopherol. It is important to note that, between 180 and 240 min, the level of α-tocopherol in liposomes loaded with the higher concentration approaches that of the initial level in liposomes loaded with the lower concentration of α-tocopherol. This is approximately the time when levels of photooxidation products start to increase rapidly (Figure 3).

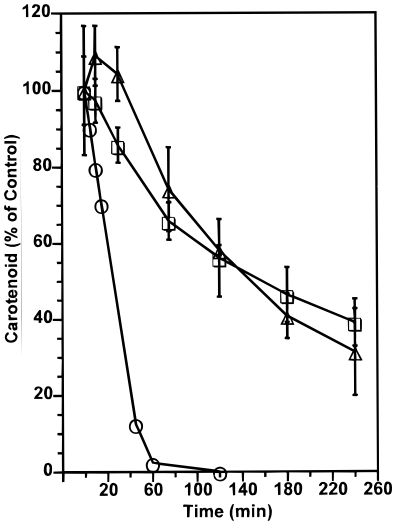

FIGURE 4: Depletion of carotenoids from photooxidized liposomes. DLPC liposomes containing either 0.45 mol % β-carotene (□), 0.45 mol % β-carotene + α-tocopherol (△), and 0.45 mol % β-carotene-5,8-endoperoxide (○) were photooxidized with methylene blue. Carotenoids were extracted and analyzed with reverse-phase HPLC as described in Experimental Procedures. Results are expressed as percent of carotenoid present in liposomes at time 0 (mean ± SD, $n = 3$).

Effect of Cumene Hydroperoxide on Type I vs Type II Photooxidation in DLPC Liposomes. The accumulation of hydroperoxides may contribute to radical-mediated lipid peroxidation by chain-branching mechanisms (Halliwell & Gutteridge, 1989). We hypothesized that hydroperoxides accumulated during Type II oxidation may undergo decomposition to radicals by the excited-state photosensitizer and that this may account for the enhanced formation of 9′-OOH over 10′-OOH during late-stage oxidation in Figure 3A. To test this hypothesis, we added cumene hydroperoxide (0.45 mol %) to DLPC liposomes prior to methylene blue-sensitized photooxidation. Cumene hydroperoxide stimulated production of 9′-OOH but not 10′-OOH during the early stages of the experiment as compared to control liposomes (Figure 3D, Table 2). When this experiment was repeated in the absence of light, no photooxidation products were formed (data not shown). This suggests that accumulation of hydroperoxides should stimulate radical-mediated lipid peroxidation (Type I oxidation) under photooxidizing conditions.

Evaluation of β-Carotene-5,8-endoperoxide as a Marker for Singlet Oxygen Quenching in Photooxidized DLPC Liposomes Containing β-Carotene. β-Carotene-5,8-endoperoxide was found to be specifically formed by singlet

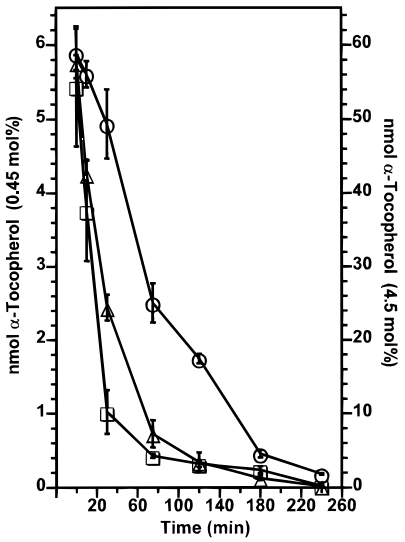

FIGURE 5: Depletion of α-tocopherol from photooxidized liposomes. DLPC liposomes containing 0.45 mol % α-tocopherol (□), 0.45 mol % α-tocopherol + β-carotene (△), and 4.5 mol % α-tocopherol (○) were photooxidized with methylene blue. α-Tocopherol was extracted and analyzed with GC-MS as described in Experimental Procedures. Results are expressed as mean ± SD, (n = 3).

oxygen oxidation of β-carotene in homogeneous solution (Stratton et al., 1993). Formation of this product during liposome photooxidation could be used as a chemical marker for singlet oxygen quenching by β-carotene in membranes. APCI LC-MS can provide rapid identification and quantification of β-carotene oxidation products (Liebler & McClure, 1996). To detect this product, photooxidized liposomes containing 0.45 mol % β-carotene were analyzed by APCI LC-MS as described above. Liposomes were analyzed for β-carotene-5,8-endoperoxide at 0, 5, 10, 15, 45, 60, and 120 min of oxidation, by selected ion monitoring at *m/z* 569 ($[M + H]^+$) following calibration with standards of β-carotene and β-carotene-5,8-endoperoxide. However, this product was not observed even at sensitivity levels in the range of 1−20 fmol.

The absence of β-carotene-5,8-endoperoxide may be due to rapid breakdown under the conditions of photosensitized oxidation. To evaluate the stability of this product, DLPC liposomes were loaded with 0.45 mol % β-carotene-5,8-endoperoxide and photooxidized with methylene blue. Depletion of β-carotene-5,8-endoperoxide was analyzed by HPLC (Figure 4). These data indicate that β-carotene-5,8-endoperoxide is rapidly depleted under these conditions and may explain why it was not detected in the above experiments.

DISCUSSION

Here we report the application of a specific assay for free radical and singlet oxygen-dependent lipid peroxidation to studies of photosensitized membrane oxidation. Other assays measure lipid peroxidation both directly and indirectly and include UV−vis analysis of conjugated dienes, the thiobarbituric acid-reactive substances test (TBARS), and GC or HPLC techniques. However, these assays are unable to quantitatively distinguish between radical-induced and singlet oxygen-induced lipid peroxidation. In this study, a new method for quantitative determination of nonspecific vs Type II-mediated photooxidation products in liposomes was developed based on the production of quantitative standards of 9- and 10-OH MeLin and their trideuterolabeled analogues. This method offers femtomole sensitivity and distinguishes between radical-mediated and singlet oxygen-specific lipid peroxidation. We have used this assay to characterize the contribution of Type I and Type II oxidative processes to photosensitized oxidations of lipid bilayers and the mechanisms of photoprotection by the antioxidants α-tocopherol and β-carotene. Our results clearly indicate the complementary nature of these antioxidants in protecting against Type I and Type II oxidative processes, respectively.

The photooxidation products of the linoleoyl moiety of DLPC are well characterized (van Kuijk et al., 1985; Terao et al., 1981). Standards of the methyl esters of these products can be synthesized and reduced to stable hydroxides, as demonstrated by Thomas and Pryor (1980). The four products of this reaction are 9-, 10-, 12-, and 13-OH positional isomers. Normal-phase HPLC analysis of the product mixture does not adequately resolve the 12- and 13-OH isomers, whereas baseline resolution of 9- and 10-OH isomers was achieved (Figure 1). This is consistent with previous studies on photooxidized linoleate methyl ester (Thomas & Pryor, 1980; Chacon et al., 1987). Type I photooxidation of DLPC forms equal amounts of 9′- and 13′-OOH, while Type II photooxidation forms equal amounts of all four isomers. Since these processes form equal amounts of their respective isomers, levels of 9′- and 10′-OOH serve as indices of nonspecific and Type II-mediated photooxidation, respectively.

Absolute quantification of purified 9- and 10-OH MeLin (and their trideuterated analogues) was achieved with a combination of UV-vis and GC-FID. 9-OH MeLin contains a strongly absorbing conjugated diene chromophore and can be quantified with UV−vis spectroscopy based on published extinction coefficients (Chan & Levett, 1977). The 10-OH isomer does not contain a conjugated diene and quantification based only on the weakly absorbing carbonyl is unreliable, since the absorbance maximum of this functional group is near or below the UV cutoff of most solvents. FID responds proportionately to the number of $-CH_2-$ groups introduced into the flame (Willard et al. 1988). Since 9- and 10-OH MeLin vary only in the position of the hydroxyl group, FID detector response to equal amounts of these compounds is assumed to be equivalent, within experimental error. This assumption was used in a previous study of fatty acid methyl ester quantification by Onkenhout et al. (1995). Thus, stock solutions of 10-OH MeLin can be quantified by GC-FID using calibration curves based on known amounts of 9-OH MeLin. Deuterium-labeled 9- and 10-OH MeLin, prepared by transesterification with methanol-d_4 and quantified with GC-FID, serve as internal standards for GC-MS analysis of these compounds.

GC-MS analysis of hydroxylinoleate methyl ester isolated from photooxidized DLPC liposomes is simplified by saturation of the double bonds prior to analysis. Specific detection of 9-OH MeLin with GC-MS is difficult since TMS ethers of 9- and 13-OH MeLin are not completely resolved, and both show fragment ions at *m/z* 225 and 311 (Lehmann et al., 1992). Hydrogenation of products eliminates this problem since TMS ethers of hydroxystearate methyl ester isomers all have isomer-specific fragment masses (Chart 1). Catalytic hydrogenation was adapted from the method of Lehmann et al. (1992), in which products are subjected to hydrogenation with platinum oxide/H_2 *after* TMS derivati-

Chart 1: Key Electron-Ionization MS Fragment Ions of 9- and 10-O-TMS Stearate Methyl Ester[a]

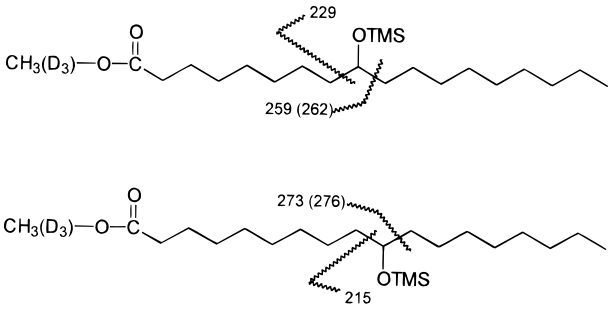

[a] Specific carboxy-terminal fragment ions for 9-O-TMS stearate methyl ester (*m/z* 259) and 10-O-TMS stearate methyl ester (*m/z* 273) were monitored along with corresponding ions for trideuterated internal standards (*m/z* 262 and *m/z* 276).

zation. This simplifies sample preparation by eliminating platinum oxide filtration steps and preventing possible interference of the platinum oxide with BSTFA derivatization.

Selected ion monitoring of characteristic fragment ions of methyl stearate TMS ethers is sensitive and specific for the positional isomers of interest. Since fragment ions are characteristic of their respective compounds, coelution of the other oxidation products is not a problem. Fragmentation patterns for the final derivatized products 9- and 10-O-TMS stearate methyl ester are shown in Chart 1.

Application of this assay permitted evaluation of the divergence in Type I and Type II processes in photooxidations. Photooxidation of DLPC liposomes by methylene blue showed a parallel time-dependent increase in 9′- and 10′-OOH as expected (Figure 2). However, levels of 9′-OOH increased faster than 10′-OOH at later time points. This divergence can be interpreted as a shift in oxidative processes from singlet oxygen-mediated photooxidation (Type II) to radical-induced lipid peroxidation (Type I). It thus appears that Type II mechanisms prevail in early stages of methylene blue-sensitized lipid peroxidation, whereas radical-mediated processes are responsible for a greater fraction of lipid peroxidation at later stages. A buildup of lipid hydroperoxides at early stages may enhance Type I photooxidation at later stages (Scheme 2). Lipid hydroperoxides may readily undergo secondary reactions with excited-state sensitizer (or possibly O_2^-) to form radicals that can initiate lipid peroxidation via Type I mechanisms (Scheme 2). Following initiation, propagation of lipid peroxidation chain reactions is pO_2-dependent, not photosensitizer-dependent. Thus, levels of radical-mediated products may increase rapidly at later stages of lipid peroxidation.

Products formed by secondary decomposition of lipid hydroperoxides are no longer detectable by this assay. Thus, at very late stages these results suggest that hydroperoxide products are decreasing when overall oxidation actually is increasing (Figure 2A). High levels of lipid hydroperoxides may compete for radicals due to the facile loss of the hydroperoxide hydrogen (Porter et al., 1995; Dix & Aikens, 1993).

Simultaneous measurement of singlet oxygen-specific and nonspecific lipid peroxidation is useful in determining a photooxidation profile of photosensitizing agents. Methylene blue causes more singlet oxygen-mediated lipid peroxidation than TPP does in this system. Rose Bengal and its

Scheme 2: Mechanisms of Photosensitizer-Induced Lipid Peroxidation at Early and Late Stages[a]

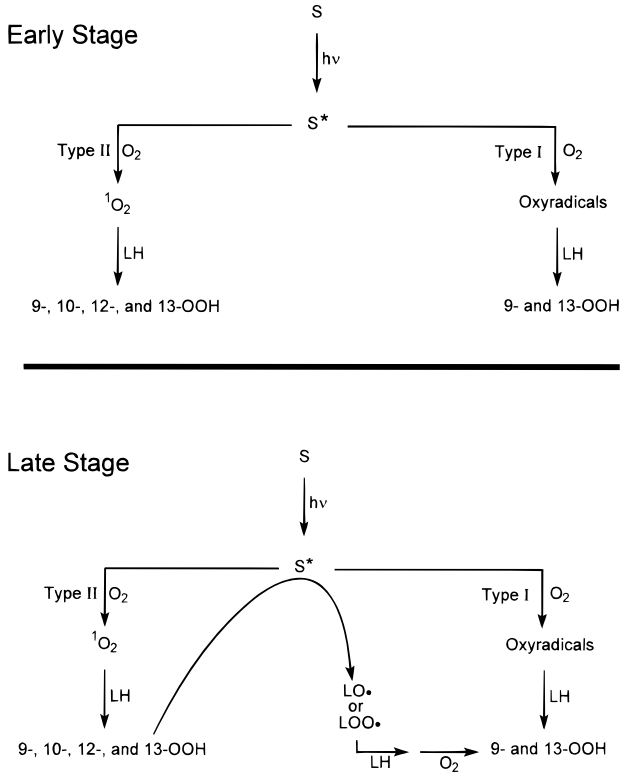

[a] Excited-state sensitizer (S*) catalyzes Type I and Type II photooxidation. At later stages, lipid hydroperoxides produced by Type II mechanisms may accelerate radical-mediated lipid peroxidation by undergoing sensitizer-induced decomposition to radicals (LO• and LOO•).

triethylammonium salt generated comparable amounts of 9′- and 10′-OOH, although the yield of products was curtailed, especially after 30 min. This result is probably due to the rapid bleaching of photosensitizer that was observed in these experiments. The observed differences in product distribution presumably reflect differences in the properties of the excited-state sensitizers.

A particularly interesting finding of this work is the shift from Type II to Type I photooxidation with time in methylene blue-sensitized photooxidations. We postulated that this shift resulted from the accumulation of lipid hydroperoxides from Type II lipid oxidation, which then reacted with the excited sensitizer to form free radicals (Scheme 2). The resulting radicals then initiate free radical autoxidation, which generates excess 9′-OOH via chain-carrying peroxyl radicals. To test this hypothesis, we performed methylene blue-sensitized photooxidations in liposomal suspensions supplemented with cumene hydroperoxide. GC-MS analysis indicated that cumene hydroperoxide stimulated the formation of 9′-OOH but not that of 10′-OOH. This pattern reflects increased radical oxidation of the DLPC and is consistent with excited photosensitizer-dependent decomposition of hydroperoxide to free radicals. This interpretation is further supported by the absence of a cumene hydroperoxide-stimulated formation of 9′-OOH in dark controls. It is also possible that increased radical formation may be due in part to breakdown of hydroperoxide by transition metal contaminants in the reaction medium. However, this seems unlikely to account for the magnitude of the stimulatory effect observed with cumene hydroper-

oxide, as the availability of metal catalyst rather than that of the hydroperoxide would be rate-limiting in this system. Nevertheless, even in photooxidations occurring exclusively by a Type II mechanism, some excess of 9′-OOH would be expected due to the combined effects of (1) transition metal contamination, (2) sensitizer-induced decomposition of hydroperoxide product, and (3) possible artifactual autoxidation during sample workup.

Although β-carotene is an effective antioxidant in photosensitized oxidations, the relative contributions of singlet oxygen quenching and radical scavenging have not been quantified. Application of the GC-MS assay described here provides a unique means of assessing the mechanisms of antioxidant action for β-carotene and α-tocopherol. As shown by the data in Table 2 and Figure 3, β-carotene inhibited photooxidation in this system. β-Carotene equally suppressed the formation of both 9′-OOH and 10′-OOH as compared to control. This indicates that β-carotene acted almost exclusively to suppress Type II oxidation. Since β-carotene effectively suppressed virtually all photooxidation for the first 75 min of the experiment, methylene blue photooxidation in this system appears to work mainly via a Type II mechanism. This is consistent with previous studies indicating Type II mechanisms in methylene blue-sensitized photooxidations (Frankel et al., 1979; Ojima et al., 1993; Terao et al., 1981). However, the accumulation of small amounts of hydroperoxide products led to enhanced 9′-OOH formation, even when a significant fraction of the β-carotene was present. This divergence in the slopes of the photooxidation product curves after 75 min indicates an increase in Type I (radical-mediated) photooxidation. This result indicates that although β-carotene effectively suppresses Type II oxidations, small amounts of hydroperoxides nevertheless lead to significant increases in Type I oxidation, which was not effectively suppressed. Indeed, the higher the contribution of Type I mechanisms, the less effective β-carotene would be in suppression of photooxidation. This is supported by previous studies in our laboratory that showed β-carotene to be a poor antioxidant in lipid bilayers undergoing exclusive radical-mediated oxidation at high pO_2 (Kennedy & Liebler, 1992; Liebler et al., 1997).

α-Tocopherol displayed a strikingly different antioxidant profile in these experiments. α-Tocopherol is a highly effective radical chain-breaking antioxidant but is 100-fold less effective than β-carotene as a singlet oxygen quencher (Foote, 1979), though recent studies have shown the effectiveness of α-tocopherol as a singlet oxygen quencher may vary with the membrane microenvironment (Fukuzawa et al., 1997). Photooxidation was not suppressed by 0.45 mol % α-tocopherol in this system (Table 2). The divergence between curves of 9′-OOH and 10′-OOH suggested that α-tocopherol was not effective in suppressing radical-mediated lipid peroxidation after 75 min (Figure 3). However, GC-MS analyses indicated that >90% depletion of α-tocopherol had occurred by 75 min of photooxidation (Figure 5). A 10-fold increase in α-tocopherol concentration to 4.5 mol % suppressed all photooxidation from 0 to 75 min. Photooxidation increased gradually from 75 to 240 min with only a minimal difference between the amounts of 9′- and 10′-OOH produced, indicating that Type I photooxidation was almost completely suppressed (Figure 3). α-Tocopherol levels remained high enough to almost completely suppress singlet oxygen-mediated lipid peroxidation for the first 2 h and suppress radical-mediated lipid peroxidation throughout the experiment. These data indicate that, at physiologic concentrations in the lipid bilayer [*e.g.*, 0.05−0.2 mol % (Sevanian et al., 1982; Kornbrust & Mavis, 1980)], α-tocopherol is a relatively ineffective quencher of singlet oxygen and is instead readily consumed. Thus, antioxidant actions of α-tocopherol in photosensitized oxidations are probably confined to free radical scavenging and suppression of Type I reactions.

Interestingly, the presence of equimolar β-carotene did not prevent α-tocopherol depletion. In liposomes containing both antioxidants, neither significantly affected the depletion of the other. Similarly, equimolar α-tocopherol did not enhance suppression of photooxidation by β-carotene when both antioxidants were present. Photooxidation product levels were actually slightly higher than levels seen when β-carotene alone was present (Table 2). This result may reflect some mild prooxidant interaction of the two antioxidants at the elevated oxygen tension used in our experiments. Alternatively, one antioxidant may have altered the membrane distribution or microenvironment of another, thus affecting antioxidant performance. The lack of a synergistic antioxidant interaction is somewhat surprising given that β-carotene would be expected to prevent singlet oxygen-dependent α-tocopherol oxidation. However, differences in α-tocopherol and β-carotene depletion kinetics suggest that the two antioxidants may not have the same degree of interaction with oxidants in this system. The results show that α-tocopherol was consumed much faster than β-carotene. This is consistent with the results of Oshima et al. (1993). Our HPLC analyses of β-carotene consumption indicated that only 35% of the β-carotene was depleted by 75 min. It is possible that the β-carotene present in the reaction system may not be as completely distributed throughout the liposome membrane as α-tocopherol. Due to the hydrophobic nature of β-carotene, microcrystalline aggregates may be formed in suspension or within the bilayer during liposome preparation (Kennedy & Liebler, 1992). Aggregates in suspension, which may be essentially inert toward reactions with lipid molecules, would still appear in carotenoid extracts from liposomes and may be responsible for the apparent stability of β-carotene indicated by the data in Figure 4.

Singlet oxygen oxidation of β-carotene forms β-carotene-5,8-endoperoxide (Stratton et al., 1993). This product is specific for singlet oxygen oxidation and was prepared by us as a marker for this action. Quantification of this marker product in complex systems would provide an index of singlet oxygen quenching by β-carotene. Due to chromatographic and spectroscopic similarities with other oxidation products, LC-MS is the method of choice for analysis of this compound, as it provides a high degree of specificity and sensitivity. However, APCI LC-MS analysis failed to detect this product in the reaction mixture. To test the stability of this product, DLPC liposomes were loaded with 0.45 mol % β-carotene-5,8-endoperoxide and photooxidized with methylene blue. Figure 4 indicates that this product is much less stable than β-carotene under these conditions, probably due to decomposition caused by lipid radical intermediates formed during lipid peroxidation. However, this does not mean that this product should be dismissed as a biomarker for singlet oxygen activity in biological systems. Stability of this compound appears to be environment-dependent. In contrast to the liposome system, β-carotene-

5,8-endoperoxide was easily isolated from the solution model where harsh photooxidation conditions existed (Stratton et al., 1993). In living systems the stability of this compound may be enhanced by membrane microenvironment, positioning, or the presence of other biomolecules in the membrane. The utility of β-carotene-5,8-endoperoxide as a biomarker is therefore unresolved.

In conclusion, application of a new GC-MS assay made it possible to dissect the contributions of Type I and Type II reactions to photosensitized oxidations of lipid bilayers. β-Carotene was a highly effective inhibitor of Type II oxidation by virtue of its effectiveness as a singlet oxygen quencher. In contrast, physiologic levels of α-tocopherol were ineffective in suppressing photosensitized oxidation, whereas at supraphysiologic concentrations, α-tocopherol suppressed both Type I and Type II-mediated oxidation. Application of this analytical approach holds promise for future studies of photosensitized oxidative injury in animal models and human studies.

ACKNOWLEDGMENT

We thank Thomas D. McClure, Ph.D., for performing mass spectral analyses, Dan Baker and Kathy Kaysen for chemical synthesis work, and Jeanne Burr for assistance with α-tocopherol analyses.

REFERENCES

Baxter, J. G., Robeson, C. D., Taylor, J. D., & Lehman, R. W. (1943) *J. Am. Chem. Soc. 65*, 918.
Burton, G. W., & Ingold, K. U. (1984) *Science 224*, 569.
Chacon, J. N., Jamieson, G. R., & Sinclair, R. S. (1987) *Chem. Phys. Lipids 43*, 81.
Chan, H. W., & Levett, G. (1977) *Lipids 12*, 99.
Dix, T. A., & Aikens, J. (1993) *Chem. Res. Toxicol. 6*, 2.
Foote, C. S. (1979) in *Singlet Oxygen* (Wasserman, H. H., & Murray, R. W., Eds.) pp 139−171, Academic Press, New York.
Foote, C. S., & Denny, R. W. (1968) *J. Am. Chem. Soc. 90*, 6233.
Frankel, E. N., Neff, W. E., & Bessler, T. R. (1979) *Lipids 14*, 961.
Fukuzawa, K., Matsuura, K., Tokumura, A., Suzuki, A., & Terao, J. (1997) *Free Rad. Biol. Med. 22*, 923.
Girotti, A. W. (1990) *Photochem. Photobiol. 51*, 497.
Halliwell, B., & Gutteridge, J. M. C. (1989) in *Free Radicals in Biology and Medicine*, Oxford University Press, New York.
Hubbard, W. C., Houg, A. J., Jr., Brash, A. R., Watson, J. T., & Oates, J. A. (1980) *Prostaglandins 20*, 431.
Hughes, H., Smith, C. V., Horning, E. C., & Mitchell, J. R. (1983) *Anal. Biochem. 130*, 431.
Johnson, B. E., & Ferguson, J. (1990) *Semin. Dermatol. 9*, 39.
Kennedy, T. A., & Liebler, D. C. (1991) *Chem. Res. Toxicol. 4*, 290.
Kennedy, T. A., & Liebler, D. C. (1992) *J. Biol. Chem. 267*, 4658.
Kochevar, I. E., Lambert, C. R., Lynch, M. C., & Tedesco, A. C. (1996) *Biochim. Biophys. Acta 1280*, 223.
Kornbrust, D. J., & Mavis, R. D. (1980) *Lipids 15*, 315.
Krinsky, N. I. (1979) *Pure Appl. Chem. 51*, 649.
Lehmann, W. D., Stephan, M., & Furstenberger, G. (1992) *Anal. Biochem. 204*, 158.
Liebler, D. C., & McClure, T. D. (1996) *Chem. Res. Toxicol. 9*, 8.
Liebler, D. C., Burr, J. A., Philips, L., & Ham, A. J. (1996) *Anal. Biochem. 236*, 27.
Liebler, D. C., Stratton, S. P., & Kaysen, K. L. (1997) *Arch. Biochem. Biophys. 338*, 244.
Loidl-Stahlhofen, A., Hannemann, K., & Spiteller, G. (1994) *Biochim. Biophys. Acta 1213*, 140.
Mathews-Roth, M. M. (1993) *Ann. N.Y. Acad. Sci. 691*, 127.
Mathews-Roth, M. M., Pathak, M. A., Fitzpatrick, T. B., Harber, L. C., & Kass, E. H. (1974) *J. Am. Med. Assoc. 228*, 1004.
Ojima, F., Sakamoto, H., Ishiguro, Y., & Terao, J. (1993) *Free Rad. Biol. Med. 15*, 377.
Onkenhout, W., Venizelos, V., van der Poel, P. F. H., van den Heuvel, M. P. M., & Poorthuis, B. J. H. M. (1995) *Clin. Chem. 41*, 1467.
Oshima, S., Ojima, F., Sakamoto, H., Ishiguro, Y., & Terao, J. (1993) *J. Nutr. Sci. Vitaminol. 39*, 607.
Porter, N. A., Caldwell, S. E., & Mills, K. A. (1995) *Lipids 30*, 277.
Sevanian, A., Hacker, A. D., & Elsayed, N. (1982) *Lipids 17*, 269.
Sieber, F., Spivak, J. L., & Sutcliffe, A. M. (1984) *Proc. Natl. Acad. Sci. U.S.A. 81*, 7584.
Stratton, S. P., Schaefer, W. H., & Liebler, D. C. (1993) *Chem. Res. Toxicol. 6*, 542.
Terao, J., Hirota, Y., Kawakatsu, M., & Matsushita, S. (1981) *Lipids 16*, 427.
Thomas, M. J., & Pryor, W. A. (1980) *Lipids 15*, 544.
van Kuijk, F. J., Thomas, D. W., Stephens, R. J., & Dratz, E. A. (1985) *J. Free Rad. Biol. Med. 1*, 215.
Willard, H. H., Merritt, L. L., Jr., Dean, J. A., & Settle, F. A., Jr. (1988) in *Instrumental Methods of Analysis*, Wadsworth, Belmont, CA.

BI9708646